

# Ba<sub>1-x</sub>Na<sub>x</sub>Ti<sub>2</sub>Sb<sub>2</sub>O (0.0 ≤ x ≤ 0.33): A Layered Titanium-Based Pnictide Oxide Superconductor

Phuong Doan,<sup>†,§</sup> Melissa Gooch,<sup>‡,§</sup> Zhongjia Tang,<sup>†,§</sup> Bernd Lorenz,<sup>‡,§</sup> Angela Möller,<sup>†,§</sup> Joshua Tapp,<sup>†,§</sup> Paul C. W. Chu,<sup>‡,§,||</sup> and Arnold M. Guloy<sup>\*,†,§</sup>

<sup>†</sup>Department of Chemistry, <sup>‡</sup>Department of Physics, and <sup>§</sup>Texas Center for Superconductivity, University of Houston, Houston, Texas 77204, United States

<sup>||</sup>Lawrence Berkeley National Laboratory, 1 Cyclotron Road, Berkeley, California 94720, United States

## S Supporting Information

**ABSTRACT:** A new layered Ti-based pnictide oxide superconductor, Ba<sub>1-x</sub>Na<sub>x</sub>Ti<sub>2</sub>Sb<sub>2</sub>O (0.0 ≤ x ≤ 0.33), is reported. X-ray studies revealed that it crystallizes in the tetragonal CeCr<sub>2</sub>Si<sub>2</sub>C structure. The undoped parent compound, BaTi<sub>2</sub>Sb<sub>2</sub>O [P4/mmm; a = 4.1196(1) Å; c = 8.0951(2) Å], exhibits a charge density wave (CDW)/spin density wave (SDW) transition at 54 K. Upon chemical doping with Na, the CDW/SDW transition is systematically suppressed, and superconductivity arises with the critical temperature (T<sub>c</sub>) increasing to 5.5 K. Bulk superconductivity was confirmed by resistivity, magnetic, and heat capacity measurements. Like the high-T<sub>c</sub> cuprates and the iron pnictides, the superconductivity in BaTi<sub>2</sub>Sb<sub>2</sub>O arises from an ordered state. Similarities and differences between BaTi<sub>2</sub>Sb<sub>2</sub>O and the cuprate and iron pnictide superconductors are discussed.

The discovery of superconductivity in iron pnictides and chalcogenides sparked immense activity in the field of high-temperature superconductivity and revitalized the interest in layered transition-metal oxides, chalcogenides, and pnictides.<sup>1</sup> The proximity of spin and/or charge ordering in intrinsic compounds to a superconducting ground state emerging through carrier doping appears to be a common feature of unconventional superconductors, including cuprates and heavy fermions (antiferromagnetism), iron pnictides [spin density wave (SDW)], and layered chalcogenides [charge density wave (CDW)].<sup>2-4</sup> Low-dimensional metallic systems are susceptible to electronic instabilities, such as CDW or SDW formation, which occur when their Fermi surfaces are nested.<sup>5</sup> Nesting occurs when large areas of the Fermi surface are nearly parallel (i.e., separated only by a characteristic vector **q** in reciprocal space), which leads to an instability with a long-range order of spins or charges. The competition and mutual interaction of these different orderings in strongly correlated systems is a foundation for novel physics (e.g., spin-fluctuation-mediated superconductivity,<sup>6</sup> quantum critical phenomena<sup>7</sup>) and provides new opportunities for exploratory materials synthesis.

On the basis of the common intrinsic behavior with the cuprate and iron pnictide superconductors, the titanium pnictide oxides Na<sub>2</sub>Ti<sub>2</sub>Pn<sub>2</sub>O (Pn = As, Sb)<sup>8</sup> have been proposed as possible candidates for new superconductors.<sup>9,10</sup> These metallic compounds are members of a wider family of

layered transition-metal pnictide oxides,<sup>10,11</sup> and they exhibit distinct phase transitions<sup>12</sup> that are associated with the formation of CDWs or SDWs.<sup>13-15</sup> The possible origin of these transitions have been discussed,<sup>16</sup> and band structure calculations revealed a nesting feature in the Fermi surface that was later found also to be associated with a periodic lattice distortion.<sup>17</sup>

Similar to the layered structures and magnetic behavior of the iron pnictides, where alkali and alkaline-earth metals form stacked layered structures with Fe<sub>2</sub>As<sub>2</sub> slabs,<sup>18,19</sup> BaTi<sub>2</sub>As<sub>2</sub>O, an alkaline-earth metal analogue of Na<sub>2</sub>Ti<sub>2</sub>Pn<sub>2</sub>O, was recently reported.<sup>20</sup> It features magnetic and resistivity anomalies similar to the transitions observed in Na<sub>2</sub>Ti<sub>2</sub>Pn<sub>2</sub>O. However, attempts to induce superconductivity in both Na<sub>2</sub>Ti<sub>2</sub>Pn<sub>2</sub>O and BaTi<sub>2</sub>As<sub>2</sub>O by chemical substitution and Li intercalation have to date been unsuccessful, although lower CDW/SDW transition temperatures were observed.<sup>20</sup>

Herein we report the synthesis of a layered titanium pnictide oxide, BaTi<sub>2</sub>Sb<sub>2</sub>O, that exhibits a CDW/SDW transition at a lower temperature, T<sub>s</sub> = 54 K. Partial substitution of Ba by Na results in a superconducting phase, Ba<sub>1-x</sub>Na<sub>x</sub>Ti<sub>2</sub>Sb<sub>2</sub>O (0.05 ≤ x ≤ 0.33), with the critical temperature (T<sub>c</sub>) reaching a maximum value of 5.5 K.

The title compounds were synthesized by high-temperature reactions of the appropriate reactants [BaO (99.5%, STREM), BaO<sub>2</sub> (95%, Sigma-Aldrich), Na<sub>2</sub>O (80% Na<sub>2</sub>O and 20% Na<sub>2</sub>O<sub>2</sub>, Sigma Aldrich), Ti (99.99%, Sigma Aldrich), Sb (pieces, 99.999%, Alfa Aesar)] in welded Nb containers within evacuated quartz jackets. The reactions were performed at 900 °C for 3 days, after which the reaction mixtures were slowly cooled (2 °C/min) to 200 °C. Additional regrinding and sintering at 900 °C for another 3 days was performed to ensure phase homogeneity. The air- and moisture-sensitive polycrystalline products had a dark-gray color. All experimental handling and physical measurements (transport, magnetic, and heat capacity) were performed under inert conditions within a purified Ar-atmosphere glovebox with total H<sub>2</sub>O and O<sub>2</sub> levels of <0.1 ppm. Details of the experimental procedures and measurements, results of the chemical analyses, X-ray crystallographic data and tables, and list of lattice parameters are given in the Supporting Information.

Received: August 8, 2012

Published: September 21, 2012

The phase purity of the resulting polycrystalline samples was investigated by powder X-ray diffraction (PXRD) (Figure 1).

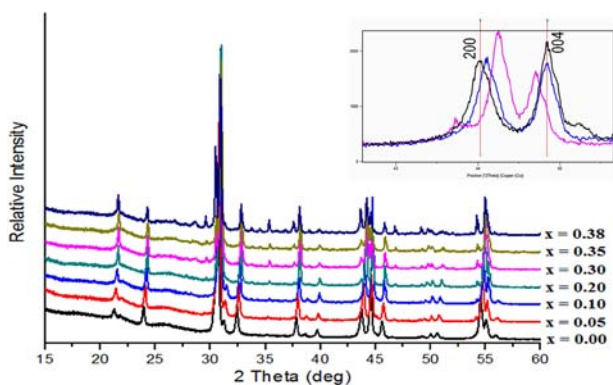


**Figure 1.** PXRD data of  $\text{Ba}_{1-x}\text{Na}_x\text{Ti}_2\text{Sb}_2\text{O}$  with  $x = 0.00$ – $0.38$ . The background at low angles arises from the scattering of the Mylar protective film. The inset shows the [200] and [004] diffraction peaks for representative samples with  $x = 0.00$  (black), 0.10 (blue), and 0.30 (pink).

The PXRD data for  $\text{BaTi}_2\text{Sb}_2\text{O}$  [ $a = 4.1196(1)$  Å;  $c = 8.0951(2)$  Å] and  $\text{Ba}_{1-x}\text{Na}_x\text{Ti}_2\text{Sb}_2\text{O}$  were refined to the  $\text{BaTi}_2\text{As}_2\text{O}$  and  $\text{CeCr}_2\text{Si}_2\text{C}$  models ( $P4/mmm$ ) by the Rietveld method using the Rietica program.<sup>21</sup> Phase analyses of the PXRD data for  $\text{Ba}_{1-x}\text{Na}_x\text{Ti}_2\text{Sb}_2\text{O}$  with  $x = 0.00$ – $0.38$  indicated that a homogeneity range exists for Na doping levels of up to 30–35%, with the formation of  $\text{Na}_2\text{Ti}_2\text{Sb}_2\text{O}$  occurring for  $x > 0.30$ . To establish the actual Na doping levels, elemental analyses of the bulk material and several crystallites of each phase-pure Na-doped polycrystalline sample were carried out by inductively coupled plasma/mass spectrometry (ICP-MS) using laser ablation. The results showed the Ba:Na molar ratio to be consistent with the nominal composition, with the Na limit of  $x = 0.33(2)$ . Moreover, the composition of the impurities for  $x > 0.30$  was also established to be  $\text{Na}_2\text{Ti}_2\text{Sb}_2\text{O}$ . No contamination from the container (Nb) was observed in any of the samples. Further analyses of the lattice parameters also showed a systematic change with increasing Na content. This was clearly reflected by the shift of the [200] peaks to higher  $2\theta$  with increasing Na content, while the [004] peaks shifted to lower values (Figure 1 inset). This is consistent with contraction along  $a$  and concomitant elongation along  $c$ .

Like  $\text{BaTi}_2\text{As}_2\text{O}$ , the title compound crystallizes in the  $\text{CeCr}_2\text{Si}_2\text{C}$  structure type, a filled variant of the  $\text{CeMg}_2\text{Si}_2$  type.<sup>22</sup> The crystal structure (Figure 2) features Ti and O atoms that form  $\text{OTi}_{4/2}$  antiperovskite layers, analogous to the  $\text{CuO}_2$  layers in the high- $T_c$  cuprates. These layers are then capped by Sb atoms above and below the empty  $\text{Ti}_4$  squares, forming  $\text{Ti}_2\text{Sb}_2\text{O}$  slabs that are stacked alternately with layers of Ba/Na atoms along the  $c$  axis. The  $\text{Ti}_2\text{Sb}_2\text{O}$  slabs are similar to  $\text{Ti}_2\text{Pn}_2\text{O}$  layers in  $\text{Na}_2\text{Ti}_2\text{Pn}_2\text{O}$ . The Ba/Na atoms lie above and below the O atoms to form an octahedral  $\text{Ti}_4(\text{Ba/Na})_2$  coordination around oxygen. Each Ti is also octahedrally coordinated by two O atoms [ $d_{\text{Ti-O}} = 2.054(1)$  Å] and four Sb atoms [ $d_{\text{Ti-Sb}} = 2.872(1)$  Å]. The network of  $\text{OTi}_{4/2}(\text{Ba/Na})_{2/2}$  octahedra is analogous to but the inverse of a  $\text{ReO}_3$ -type tetragonal perovskite, with two Sb atoms occupying cuboctahedral cavities of the antiperovskite network. However, unlike the isotypical  $\text{CeCr}_2\text{Si}_2\text{C}$ -type silicides having  $\text{Si}_2$  units with short Si interlayer distances, the Sb–Sb distances in  $\text{BaTi}_2\text{Sb}_2\text{O}$  are essentially nonbonding ( $d_{\text{Sb-Sb}} > 4.0$  Å). Upon Ba substitution

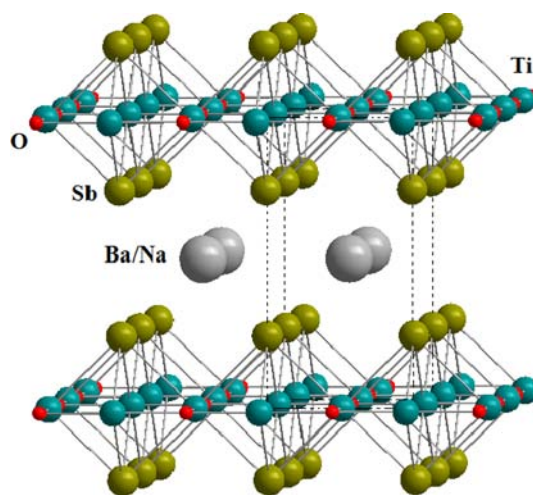


**Figure 2.** Crystal structure of  $\text{BaTi}_2\text{Sb}_2\text{O}$ . Ba, Ti, Sb, and O are shown as gray, blue, green, and red spheres, respectively.

with Na, a further expansion of the interlayer distance ( $c/2$ ) is observed, accompanied by a slight contraction of the Ti–Ti distances in the  $\text{Ti}_2\text{O}$  sheets.

The magnetic susceptibility of  $\text{BaTi}_2\text{Sb}_2\text{O}$  (Figure 3) clearly undergoes a sharp drop at  $T_s = 54$  K, indicating the onset of

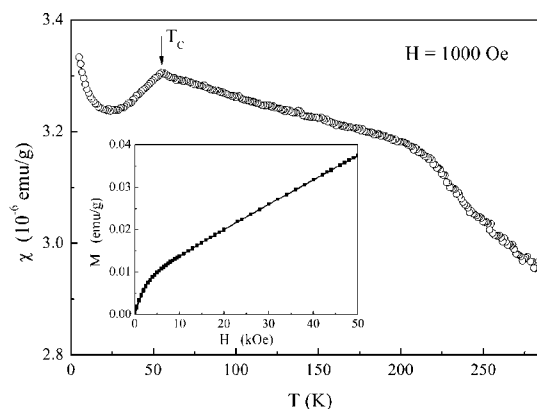


**Figure 3.** Magnetic susceptibility of  $\text{BaTi}_2\text{Sb}_2\text{O}$  as a function of temperature. Inset: field dependence of the magnetization.

magnetic ordering. Although the temperature dependence of the susceptibility is qualitatively similar to the data recently obtained for the As-based compound  $\text{BaTi}_2\text{As}_2\text{O}$ , the magnetic transition temperature of  $\text{BaTi}_2\text{Sb}_2\text{O}$  is remarkably lower ( $\sim 25\%$  of the value reported for  $\text{BaTi}_2\text{As}_2\text{O}$ ).<sup>20</sup> A similar trend of lower magnetic  $T_s$  with increasing pnictide ionic radius (As  $\rightarrow$  Sb) was also observed in the Na-based compounds  $\text{Na}_2\text{Ti}_2\text{Pn}_2\text{O}$ , with  $T_s = 320$  K for Pn = As and 120 K for Pn = Sb.<sup>14</sup> The nearly linear  $T$  dependence of the susceptibility ( $\chi$ ) above  $T_s$  is consistent with the data for  $\text{BaTi}_2\text{As}_2\text{O}$  and  $\text{Na}_2\text{Ti}_2\text{Pn}_2\text{O}$ . There is an apparent slope change for  $\chi(T)$  near 220 K, the origin of which has not yet been investigated.

The resistivity of  $\text{BaTi}_2\text{Sb}_2\text{O}$  at zero field and in magnetic fields of up to 50 kOe is shown in Figure 4 (main panel and upper inset). The sharp slope change at  $T_s = 54$  K followed by a hump is a clear indication of a CDW/SDW transition, similar to those reported for  $\text{Na}_2\text{Ti}_2\text{Sb}_2\text{O}$  and  $\text{BaTi}_2\text{As}_2\text{O}$ .<sup>17,20</sup> The resistivity in magnetic fields of 50 kOe increased by 14% at low temperatures (Figure 4, lower inset). The features that

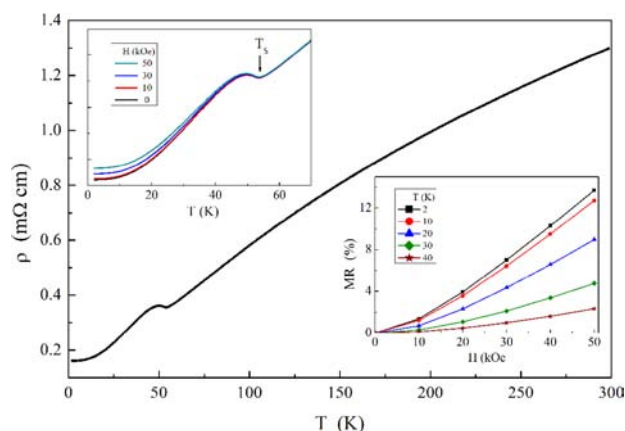


**Figure 4.** Resistivity and magnetoresistance (MR) of  $\text{BaTi}_2\text{Sb}_2\text{O}$ .

distinguish  $\text{BaTi}_2\text{Sb}_2\text{O}$  from the other pnictide oxides are the significantly lower  $T_s$  and the much larger magnetoresistance, which exceeds the reported value for  $\text{BaTi}_2\text{As}_2\text{O}$  at 50 kOe by a factor of 5.<sup>20</sup> This indicates strong coupling between the SDW state and the charge carriers, leading to a lower energy scale of the CDW/SDW state and a higher sensitivity of the low-temperature state to magnetic fields. Thus, the possibility that superconductivity could be induced with proper doping is enhanced, similar to the case of the pnictide and chalcogenide superconductors.

Substitution of Ba by Na in  $\text{BaTi}_2\text{Sb}_2\text{O}$  corresponds to a "hole" (p-type) doping of the  $\text{Ti}_2\text{Sb}_2\text{O}$  layers. As shown in Figure 5, the CDW/SDW transition temperature  $T_s$  decreases

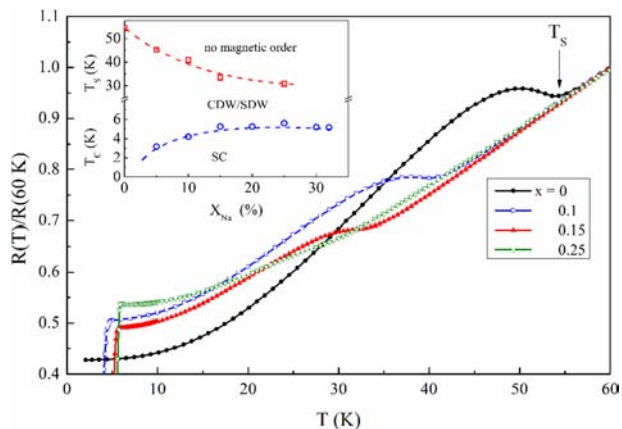


**Figure 5.** Normalized resistance of  $\text{Ba}_{1-x}\text{Na}_x\text{Ti}_2\text{Sb}_2\text{O}$  near the CDW/SDW transition. The inset shows the phase diagram derived from resistivity and magnetization measurements.

with increasing Na content ( $x$ ), from 54 K ( $x = 0$ ) to 30 K ( $x = 0.25$ ). Also,  $T_s$  does not extrapolate to zero up to a Na solubility limit of  $\sim 33\%$ , although the size of the humplike anomaly does significantly decrease with  $x$ . More importantly, the sharp drop of the resistivity to zero indicates the emergence of superconductivity at lower temperatures. The superconducting phase diagram together with the CDW/SDW transition line is summarized in the Figure 5 inset.

The superconducting state of  $\text{Ba}_{1-x}\text{Na}_x\text{Ti}_2\text{Sb}_2\text{O}$  was confirmed by a diamagnetic signal whose onset was used to define the superconducting critical temperature  $T_c$ . Figure 6 shows the zero-field-cooled (ZFC) and field-cooled (FC) magnetization data for selected Na-doped samples measured at

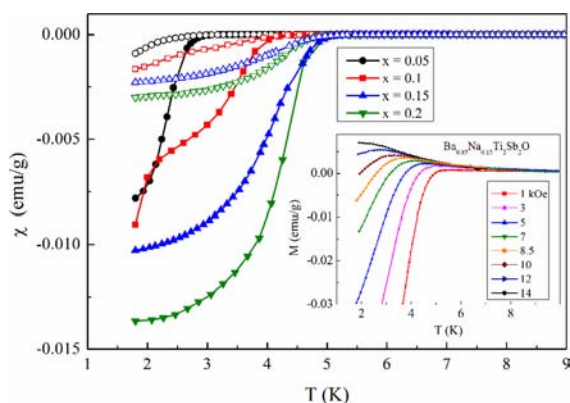


**Figure 6.** Low-temperature magnetic susceptibility of  $\text{Ba}_{1-x}\text{Na}_x\text{Ti}_2\text{Sb}_2\text{O}$  for selected values of  $x$ . Open and solid symbols refer to FC and ZFC data, respectively. The inset shows the field dependence of the magnetization at 5 K for  $x = 0.15$  under FC conditions.

10 Oe.  $T_c$  increased rapidly between  $x = 0.05$  and 0.15 and reached a plateau at higher  $x$  values. The diamagnetic signal also increased, reaching its maximum at  $x = 0.15$ . High-field FC magnetization measurements for  $x = 0.15$  (Figure 6 inset) also revealed the suppression of  $T_c$  with increasing field.

The bulk nature of the superconducting transition in  $\text{Ba}_{1-x}\text{Na}_x\text{Ti}_2\text{Sb}_2\text{O}$  was confirmed by a distinct anomaly in the constant-pressure heat capacity ( $C_p$ ), as shown in Figure 7 for  $x$

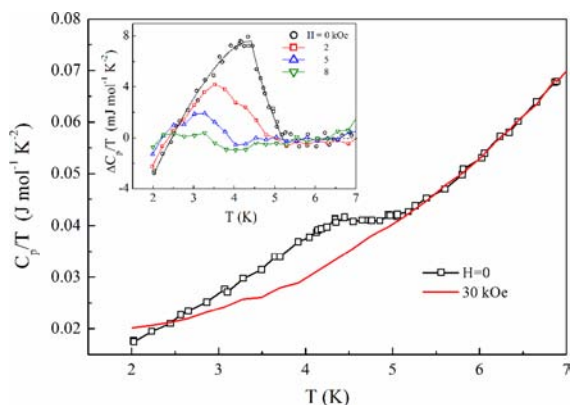


**Figure 7.** Low-temperature heat capacity of  $\text{Ba}_{0.85}\text{Na}_{0.15}\text{Ti}_2\text{Sb}_2\text{O}$ . The inset shows the difference between the heat capacities of the superconducting and normal states.

$= 0.15$ . The superconducting contribution, defined as the difference between the superconducting and normal-state  $C_p$  values [i.e.,  $\Delta C_p(H) = C_p(H) - C_p(30 \text{ kOe})$ ], was clearly resolved by subtracting the  $C_p$  data measured in magnetic fields above  $H_{c2}$  (see the Figure 7 inset). The  $C_p$  peak shifted to lower temperature with increasing field, as expected for a superconducting transition. The jump in the heat capacity,  $\Delta C_p/T_c = 8 \text{ mJ mol}^{-1} \text{ K}^{-2}$ , is comparable to values reported for doped iron arsenides.<sup>23</sup>

The heat capacity and magnetization data with a large diamagnetic signal provide convincing evidence that a bulk superconducting state is achieved in  $\text{BaTi}_2\text{Sb}_2\text{O}$  with Na substitution. Thus, we have found a new layered Ti-based pnictide oxide wherein a superconducting state arises from a magnetically ordered state when properly doped, akin to the high- $T_c$  cuprates and iron pnictides.

Although the transition temperatures in Na-doped  $\text{BaTi}_2\text{Sb}_2\text{O}$  are relatively low, there are significant and striking similarities with the cuprate and iron pnictide superconductors. The  $\text{Ti}_2\text{O}$  square nets in  $\text{BaTi}_2\text{Sb}_2\text{O}$  are inverse to the  $\text{CuO}_2$  planes in the cuprates. Moreover, Ti is formally trivalent with a  $d^1$  configuration, analogous to the “hole”  $d^9$  configuration of Cu in the cuprates. In addition, the Sb atoms bonded to Ti atoms above and below the  $\text{Ti}_2\text{O}$  planes contribute significantly to the magnetic superexchange between the Ti spins,<sup>12</sup> which resembles the electronic situation in the superconducting iron pnictides. The existence of a nesting property of the Fermi surface of undoped pnictide oxide compounds<sup>12</sup> and the associated CDW/SDW instability accompanied by a structural distortion<sup>14</sup> is another feature that has been observed in the iron pnictides. More importantly, superconductivity emerges from the magnetically ordered state upon doping, and the CDW/SDW transition temperature  $T_s$  is suppressed to lower temperatures. However, in contrast to the iron pnictides, the CDW/SDW state survives at relatively higher doping levels (Figure 5 inset). Unfortunately, the solubility of Na in  $\text{BaTi}_2\text{Sb}_2\text{O}$  was limited at  $\sim 33\%$ , and the phase diagram could not be extended beyond this limit. The softening of the resistivity anomaly at  $T_s$  with higher Na content (Figure 5) may also indicate an abrupt disappearance of the CDW/SDW phase above a critical doping level, similar to the phase diagram of  $\text{LaO}_{1-x}\text{F}_x\text{FeAs}$ .<sup>24</sup>

In view of the unsuccessful attempts to induce superconductivity in  $\text{BaTi}_2\text{As}_2\text{O}$ <sup>17</sup> and the relatively low Na content (5%) needed to induce the superconducting state in  $\text{BaTi}_2\text{Sb}_2\text{O}$ , a question arises about the major differences between doping in  $\text{BaTi}_2\text{As}_2\text{O}$  and in  $\text{BaTi}_2\text{Sb}_2\text{O}$ . One significant difference between the two parent compounds is the much lower energy scale of the CDW/SDW phase in  $\text{BaTi}_2\text{Sb}_2\text{O}$ , which results in the lowest transition temperature ( $T_s = 54$  K) among all Ti-based pnictide oxides. Since the competition between magnetic order and superconductivity is a crucial element in unconventional superconductivity, it is conceivable that this lower energy scale is the key to making superconductivity emerge upon doping with Na in  $\text{BaTi}_2\text{Sb}_2\text{O}$ . Further work will focus on exploring the detailed phase diagram of the new superconductors, the nature of the CDW/SDW phase, and the emerging superconductivity in  $\text{BaTi}_2\text{Sb}_2\text{O}$ . Exploratory syntheses of other layered Ti-based pnictide oxide superconductors and related compounds may yet lead to new families of unconventional superconductors.

## ■ ASSOCIATED CONTENT

### ■ Supporting Information

Experimental procedures, results of the elemental analyses, summary of crystallographic data, and a list of lattice parameters and their trends. This material is available free of charge via the Internet at <http://pubs.acs.org>.

## ■ AUTHOR INFORMATION

### Corresponding Author

aguloy@uh.edu

### Notes

The authors declare no competing financial interest.

## ■ ACKNOWLEDGMENTS

This work was supported in part by the State of Texas through the Texas Center for Superconductivity, the U.S. Air Force

Office of Scientific Research, the National Science Foundation (CHE-0616805), and the R. A. Welch Foundation (E-1297). P.C.W.C. acknowledges the TLL Temple Foundation, the J. J. and R. Moores Endowment, and LBNL through the U.S. DOE.

## ■ REFERENCES

- (1) Paglione, J.; Greene, R. L. *Nat. Phys.* **2010**, *6*, 645–658 and references therein.
- (2) Norman, M. R. *Science* **2011**, *332*, 196–200.
- (3) Sipos, B.; Kusmartseva, A. F.; Akrap, A.; Berger, H.; Forro, L.; Tütis, E. *Nat. Mater.* **2008**, *7*, 960–965.
- (4) Morosan, E.; Zandbergen, H. W.; Dennis, B. S.; Bos, J. W. G.; Onose, Y.; Klimczuk, T.; Ramirez, A. P.; Ong, N. P.; Cava, R. J. *Nat. Phys.* **2006**, *2*, 544–550.
- (5) (a) Lomer, W. M. *Proc. Phys. Soc. London* **1962**, *80*, 489–496. (b) Wilson, J. A.; DiSalvo, F. J.; Mahajan, S. *Adv. Phys.* **1975**, *24*, 117. (c) Whangbo, M.-H.; Canadell, E. *Chem. Rev.* **1991**, *91*, 965–1034.
- (6) (a) Kohn, W.; Luttinger, J. M. *Phys. Rev. Lett.* **1965**, *15*, 524–526. (b) Santi, G.; Dugdale, S. B.; Jarlborg, T. *Phys. Rev. Lett.* **2001**, *87*, No. 247004.
- (7) (a) Si, Q.; Steglich, F. *Science* **2010**, *329*, 1161–1166. (b) von Lohneysen, H.; Rosch, A.; Vojta, M.; Wolfle, P. *Rev. Mod. Phys.* **2007**, *79*, 1015–1075.
- (8) Adam, A.; Schuster, H.-U. *Z. Anorg. Allg. Chem.* **1990**, *584*, 150–158.
- (9) Johrendt, D.; Hosono, H.; Hoffmann, R.-D.; Pöttgen, R. Z. *Kristallogr.* **2011**, *226*, 435–446.
- (10) Ozawa, T. C.; Kauzlarich, S. M. *Sci. Technol. Adv. Mater.* **2008**, *9*, No. 033003.
- (11) Brock, S. L.; Kauzlarich, S. M. *Comments Inorg. Chem.* **1995**, *17*, 213–238.
- (12) (a) Axtell, E. A., III; Ozawa, T.; Kauzlarich, S. M.; Singh, R. R. P. *J. Solid State Chem.* **1997**, *134*, 423–426. (b) Ozawa, T. C.; Kauzlarich, S. M.; Bieringer, M.; Greedan, J. E. *Chem. Mater.* **2001**, *13*, 1804–1810.
- (13) Pickett, W. E. *Phys. Rev. B* **1998**, *58*, 4335–4340.
- (14) Liu, R. H.; Tan, D.; Song, Y. A.; Li, Q. J.; Yan, Y. J.; Ying, J. J.; Xie, Y. L.; Wang, X. F.; Chen, X. H. *Phys. Rev. B* **2009**, *80*, No. 144516.
- (15) de Biani, F. F.; Alemany, P.; Canadell, E. *Inorg. Chem.* **1998**, *37*, 5807–5810.
- (16) Ozawa, T. C.; Pantoja, R.; Axtell, E. A.; Kauzlarich, S. M.; Greedan, J. E.; Bieringer, M.; Richardson, J. W., Jr. *J. Solid State Chem.* **2000**, *153*, 275–281.
- (17) Sasmal, K.; Lv, B.; Lorenz, B.; Guloy, A. M.; Chen, F.; Xue, Y. Y.; Chu, C. W. *Phys. Rev. Lett.* **2008**, *101*, No. 107007.
- (18) Tapp, J. H.; Tang, Z.; Lv, B.; Sasmal, K.; Lorenz, B.; Chu, P. C. W.; Guloy, A. M. *Phys. Rev. B* **2008**, *78*, No. 060505.
- (19) Wang, X. F.; Yan, Y. J.; Ying, J. J.; Li, Q. J.; Zhang, M.; Xu, N.; Chen, X. H. *J. Phys.: Condens. Matter* **2010**, *22*, No. 075702.
- (20) Hunter, B. Rietica: A Visual Rietveld Program. *International Union of Crystallography Commission on Powder Diffraction Newsletter*, No. 20, 1998. Also see: <http://www.rietica.org>.
- (21) (a) Pohlkamp, W. M.; Jeitschko, W. Z. *Naturforsch.* **2001**, *56b*, 1143–1148. (b) Zmii, O. F.; Gladyshevskii, E. I. *Sov. Phys. Crystallogr.* **1971**, *15*, 871.
- (22) Kim, J. S.; Stewart, G. R.; Kasahara, S.; Shibauchi, T.; Terashima, T.; Matsuda, Y. J. *Phys.: Condens. Matter* **2011**, *23*, No. 222201.
- (23) Luetkens, H.; Klaus, H.-H.; Kraken, M.; Litterst, F. J.; Dellmann, T.; Klingeler, R.; Hess, C.; Khasanov, R.; Amato, A.; Baines, V.; Kosmala, M.; Schumann, O. J.; Braden, M.; Hamann-Borrero, J.; Leps, N.; Kondrat, A.; Behr, G.; Werner, J.; Büchner, B. *Nat. Mater.* **2009**, *8*, 305–309.

## ■ NOTE ADDED IN PROOF

After final revisions were made we became aware of a related publication (*J. Phys. Soc. Jpn.* **2012**, *81*, 103706) on  $\text{BaTi}_2\text{Sb}_2\text{O}$ . The results on the SDW transition are in agreement with our work, and they report superconductivity at 1.2 K.